

# Mitigation of crosstalk effects in multi-LiDAR configurations

Axel L. Diehm, Marcus Hammer, Marcus Hebel\*, Michael Arens  
Fraunhofer Institute of Optronics, System Technologies, and Image Exploitation IOSB,  
Gutleuthausstr. 1, 76275 Ettlingen, Germany

## ABSTRACT

In this paper, we examine crosstalk effects that can arise in multi-LiDAR configurations, and we show a data-based approach to mitigate these effects. Due to the ability to acquire precise 3D data of the environment, LiDAR-based sensor systems (sensors based on “Light Detection and Ranging”, e.g., laser scanners) increasingly find their way into various applications, e.g. in the automotive sector. However, with an increasing number of LiDAR sensors operating within close vicinity, the problem of potential crosstalk between these devices arises. “Crosstalk” outlines the following effect: In a typical LiDAR-based sensor, short laser pulses are emitted into the scene and the distance between sensor and object is derived from the time measured until an “echo” is received. In case multiple laser pulses of the same wavelength are emitted at the same time, the detector may not be able to distinguish between correct and false matches of laser pulses and echoes, resulting in erroneous range measurements and 3D points. During operation of our own multi-LiDAR sensor system, we were able to observe crosstalk effects in the acquired data. Having compared different spatial filtering approaches for the elimination of erroneous points in the 3D data, we propose a data-based spatio-temporal filtering and show its results, which may be sufficient depending on the application. However, technical solutions are desired for future LiDAR sensors.

**Keywords:** LiDAR, laser scanning, mutual interference, crosstalk, spatial filtering, temporal filtering

## 1. INTRODUCTION

Autonomous driving is a topic of research that gets more and more important in recent years, with applications like coordinating mobile robots in an automated factory, or very complex scenarios like autonomous driving in real traffic. A key point is to guarantee the autonomous vehicles’ situational awareness. The knowledge of its own state and the states of other traffic participants together with the knowledge of the (fixed) environment they are moving in is mandatory for an autonomous vehicle to follow traffic laws and avoid collisions while driving from A to B. To get reliable status data, a variety of sensor systems are discussed to be placed in or on autonomous vehicles and infrastructure in future. The use of sensors with time-of-flight (TOF) measurement, such as ultrasound sonar sensors for close range or RADAR sensors for far range, is state of the art in the automotive sector to get distance information.

Due to the ability to deliver more accurate and dense range measurements independent of natural lighting conditions, LiDAR-based sensor systems increasingly find their way into military and civilian automotive applications. In order to provide a better data coverage, vehicles like (experimental) autonomous driving cars are even equipped with two or more LiDAR sensors simultaneously. This fact, in itself, raises the potential of mutual interference (crosstalk) between sensors of the same system. On the other hand, with a notable number of autonomous driving cars to be expected in future traffic scenarios, mutual interference between their LiDAR sensors is likely to occur. Mutual interferences may result in erroneous range measurements and 3D points, possibly causing abrupt stopping in front of or circumnavigating an imaginary object. Scanning LiDAR sensors can also be used to detect and track small objects, like unmanned aerial vehicles (UAVs), with some success (Hammer et al. [1]). As critical situations involving small UAVs increased in number recently, detection methods and countermeasures became a demanding task. Crosstalk effects can hinder the early detection of a UAV or imitate a non-existing one.

To mitigate crosstalk effects, the acquired point clouds have to be filtered such that noise and crosstalk points are deleted while existing small objects are kept. Having investigated spatial filtering methods, we propose our own temporal filtering

---

\*marcus.hebel@iosb.fraunhofer.de; phone +49 7243 992-323; fax +49 7243 992-299; www.iosb.fraunhofer.de

method showing good results on sequences of LiDAR data. After a review of related literature in Section 2 and a more detailed problem description in Section 3, the main methods for the data-based mitigation of crosstalk effects are described in Section 4. Experiments and results are presented in Section 5, and our conclusions can be found in Section 6.

## 2. RELATED WORK

The problem of mutual interference was a topic in the automotive RADAR community for years (e.g., Mu et al. [2], Goppelt et al. [3]) and still is in focus (Schipper et al. [4]). The EU project MOSARIM (More Safety for All by Radar Interference Mitigation) examined possibilities for the correction or mitigation of RADAR interferences during the years 2010 to 2012. A short overview of the project objectives and conducted work can be found in [5]. Among the documents emerging from MOSARIM, one particular report [6] defines several scenarios where crosstalk can occur in ordinary traffic situations. These scenarios are not specific to RADAR but apply to all TOF sensors.

Back in 1991, Hebert and Krotkov [7] reported their experience with a specific class of LiDAR systems: amplitude-modulated continuous-wave LiDAR systems (AMCW LiDAR). Such LiDAR systems derive the range to a reflecting object by means of the phase shift measured between the emitted signal and its reflection. In addition to the range measurement, AMCW LiDAR sensors can deliver a measurement of the intensity of the laser beam's reflectance. The experiments performed by Hebert and Krotkov led to the identification of four reasons for problematic effects resulting in invalid data: scanning pattern, mixed pixels, range/intensity crosstalk, and range drift. Unlike our interpretation of *crosstalk* as mutual interference between sensors, in their work the term "range/intensity crosstalk" describes the effect of range and intensity measurements not being completely independent, as reflections with lower intensity can lead to increased range noise and range shifts.

Kim et al. [8] analyzed the occurrence of mutual interferences between two pulsed LiDAR sensors of the same brand that work simultaneously. Using off-the-shelf sensors (SICK LMS-511), they tested the effects of different relative placement of the two LiDAR sensors. The experimental setup used three wood walls to surround a quadratic area where both LiDAR sensors were placed in. For each of the examined arrangements (2 x side-by-side, front-to-front, and back-to-back), both sensors operated for a period of 24 hours. Then, the resulting distances were compared with the correct distances (ground truth) measured by a single sensor in a separate 4 hours run. Coloring the correct and the erroneous measurements differently, they showed the diversity of the measured distances in 2D maps. By comparing normal and interfered distance maps, they deduced that the interferences have both temporal and spatial locality.

In recent years, the industry (sensor manufactures) became aware of the problems due to mutual interferences, as can be seen in Velodyne's patent [9] and Facet Technology Corporation's LiDAR Crosstalk Elimination Licensing Program [10], for instance. However, as long as technical solutions do not exist for currently available sensors, a data-based mitigation of crosstalk effects could still be the preferred method of choice.

Existing methods for noise removal in point clouds are candidates to filter erroneous measurements due to crosstalk. Typically, the removal of noise is a byproduct when reconstructing surfaces from 3D point clouds. For example, operators from the LOP family (LOP "Locally Optimal Projection" [11], WLOP "Weighted Locally Optimal Projection" [12]) allow reconstruction of surfaces from noisy point clouds. A detailed review and comparison of filters for noise removal in 3D point clouds is given by X.-F. Han et al. [13]. As handling of point clouds is commonly done by using software packages like the "Point Cloud Library" (PCL, [14]), filters from this library were included in their comparison as well. In Section 4 and Section 5, we evaluate the ability to handle crosstalk effects by noise removal filters, where we use two filters that are part of the PCL ("Radius Outlier Removal" filter and "Statistical Outlier Removal" filter [15]) and compare these to our own method.

Usually these filters work on a single global point cloud, and only spatial conditions are considered, like the average distance to neighboring points. However, LiDAR sensors typically generate a continuous sequence of overlapping point clouds, e.g., a sequence of range images or a sequence of 360° scans of a rotating scanner head. Hence, there exist temporal and spatial relationships between points of consecutive clouds. Adequate filters have to preserve both static parts and moving objects in a sequence of clouds, while removing erroneous points caused by detector noise or crosstalk. In this paper, we propose a spatio-temporal approach to filter a continuous sequence of point clouds by analyzing the local temporal behavior of points. Although our experiments used recorded data, the proposed method is real-time capable, since it only needs three consecutive point clouds at any time during operation.

### 3. PROBLEM DESCRIPTION

In general, a TOF sensor consists of at least one emitter-detector pair. The range between the sensor and an object in the scene is measured as shown in Figure 1: After sending out a short pulse, the detector circuit waits for a reflection (“echo”) of this pulse returning from a reflecting surface in the scene. By measuring the time between sending the pulse and receiving the echo, the distance to the reflecting surface is deduced using the propagation speed of the pulses. Knowing the sensor’s (georeferenced) position and orientation in 3D space, the position of the corresponding 3D point can be calculated. Together with a scanning operation, this measuring technique results in an accumulated 3D point cloud. If the scanning operation has repetitive elements, like rectangular scan patterns or 360° rotations of a scanner head, a *sequence of point clouds* is generated. In this paper, we mainly address 360° scans of rotating LiDAR scanner heads, but the nature of the problem and the solutions are valid for other sensor types as well.

Typical LiDAR-based sensors (e.g., laser scanners) emit short laser pulses. The reception time of the detector circuit can be limited to an interval  $[t_{\min}, t_{\max}]$  with  $t_{\min} > 0$  and  $t_{\max}$  set in dependence to the expected maximum range of the LiDAR sensor. Thus, using  $t_{\min}$  avoids echoes from very near objects, whereas  $t_{\max}$  allows cutting off the measurement in a certain distance in the current direction. In case multiple laser pulses of the same frequency are emitted by multiple emitters of emitter-detector pairs of one single LiDAR sensor or by multiple LiDAR sensors at nearly the same time, a detector may not be able to distinguish between correct and false matches of laser pulses and echoes. If a LiDAR sensor’s detector accepts a pulse or an echo not originating from its own emitter, this results in an erroneous range measurement and an erroneous 3D point. We call this situation *crosstalk* (see Figure 1).

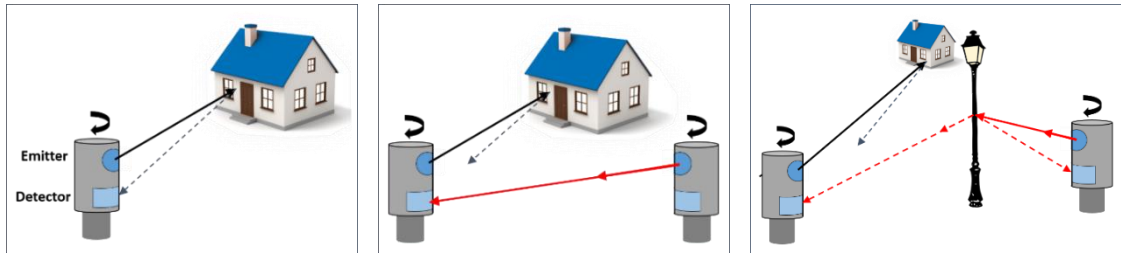


Figure 1: left: Basic principle of range detection by a TOF sensor system, shown by an exemplary LiDAR system; center: direct crosstalk scenario; right: crosstalk by reflection.

If multiple rotating scanner heads are used at the same rotation direction and frequency, similar geometrical constellations can be expected to occur within a sequence of consecutive 360° scans, yielding a couple of such erroneous 3D points in the same cloud or consecutive clouds. The deduced location of an erroneous point depends on both the reception time and the circumstances of the measurement. Some detectors are capable of acquiring multiple echoes, while others only record the first return. In the examples of crosstalk shown in Figure 1, the reception time of the false pulse/echo lies in the interval  $[t_{\min}, t_{\max}]$  before that of the correct measurement. This causes an erroneous point being placed between the correct one and the sensor. However, other constellations could also lead to erroneous points, depending on the capabilities of the detector.

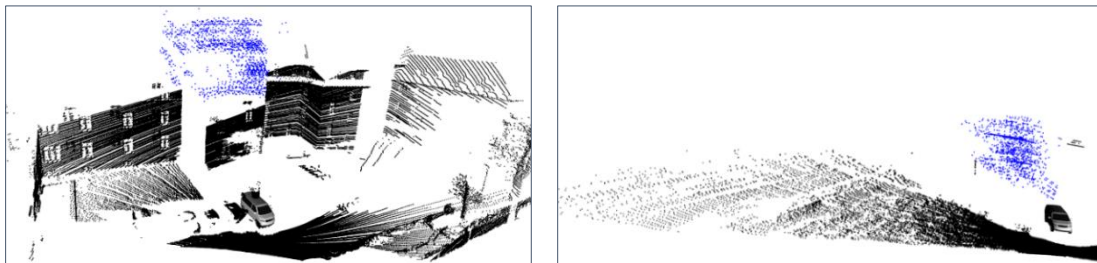


Figure 2: Examples of 3D point clouds acquired by a Velodyne HDL-64 sensor with another sensor of same type in close vicinity. Crosstalk points are shown in blue.

Using our own multi-LiDAR sensor system (see Section 5.1), we usually obtain notable numbers of clutter points in the data from time to time. As these points occur quite regularly in time and are similarly located in space, they cannot be

traced back to ordinary noise. Instead, the source of these erroneous 3D points must be crosstalk effects. Figure 2 gives an impression of this phenomenon in a building scenario (left) and in open landscape (right). It can be seen that the positions of the crosstalk points in the open landscape are closer to the sensor than those in the building scenario. Moreover, crosstalk points can be quite dense, making it hard to distinguish them from real scene objects like vegetation, cars etc. Figure 2 can be seen as a preview of the proposed method and the experiments. In the next section, we describe the method(s) to separate correctly measured 3D points and crosstalk points.

## 4. SOLUTION(S)

As mentioned above, we mainly address 360° rotating LiDAR scanners, for which the data of each 360° rotation of the scanner head can be aggregated, resulting in sequences of 3D point clouds (single scans). While noise of any kind typically occurs evenly distributed among the data points, the occurrence of crosstalk points requires specific geometrical and temporal constellations of emitted and reflected pulses between different sensors. With the majority of correctly measured 3D points in mind, an erroneous point due to crosstalk is quite a seldom event both in space and in time. However, with modern sensors that are capable of performing several millions of range measurements per second, even seldom events show an effect. Spatial and/or temporal filtering approaches are candidates to filter these erroneous measurements. First, we describe two commonly used spatial filtering methods, before we propose our own spatio-temporal filtering approach.

### 4.1 Spatial filtering

Today’s widely used software package “Point Cloud Library” (PCL, [14]) offers standard routines and filters to handle and manipulate 3D point clouds. In order to evaluate the capabilities of standard filtering methods for the removal of crosstalk points, we put two outlier removal filters of the PCL to the test: “Radius Outlier Removal” and “Statistical Outlier Removal”. Intended for the support of surface reconstruction, these filters use spatial filtering to delete noise and outliers.

#### “Radius Outlier Removal” filter

This filter counts the number of neighboring points within a sphere around each 3D point. The fixed radius of the spheres is one of the filter’s parameters. The second one is a threshold value that specifies the minimum number of neighbors to keep a point. The filter’s paradigm is to prioritize dense structures and dismiss points with less adjacent points. Using a global radius and threshold for all points is a drawback of this filter, as points close to the sensor are denser than those in far distance. It is nearly impossible to define an optimal parameterization of the filter for unevenly distributed points. If the minimum number of neighbors is set to a value greater than 2, small objects like a UAV are likely to be removed due to the few points hitting the object.

#### “Statistical Outlier Removal” filter

Another outlier removal filter in the PCL is the “Statistical Outlier Removal” [15], which assumes a Gaussian distribution of the distances between the cloud’s points. For every point in the cloud the  $k$  nearest neighboring points are determined and the average of the distances to each of its  $k$  neighbors is calculated. Then, the mean and standard deviation of all these average distances are computed. Using a parameter  $\alpha$  as multiplier for the standard deviation, threshold values around the mean are set. Every point with an average distance to its  $k$  neighbors above or below the thresholds is removed.

The filter algorithm has to process each point twice: In the first run, average distances, their mean, and their standard deviation are calculated. In the second run, noise and outliers are removed. This increases the execution time, especially with increasing amount of points in the cloud and a large value for  $k$  (number of neighbors to be considered). The filter is prone to be misguided by isolated points in larger distances (e.g., points belonging to small flying objects, noise, or crosstalk points) since these raise the calculated mean and standard deviation of the average distances such that fewer points are removed. However, a small isolated object is likely to be removed, as its average distances to the  $k$  nearest neighbors still exceeds the mean value.

### 4.2 Temporal filtering

As spatial filtering approaches process each cloud of a sequence independently, they do not take temporal relations into account that exist implicitly among consecutive clouds with overlapping content. The idea of temporal filtering is to compare a cloud  $c_t$  to preceding and succeeding clouds, i.e.,  $c_{t-1} \cup c_{t+1}$  or a broader subsequence. Scanned parts of the static background or moderately moving objects are expected to be represented by similar 3D points in consecutive clouds of a sequence. In contrast, noise or crosstalk points occur as temporally isolated events.

The comparison of an acquired point cloud to a known static background is an easy way to identify all irregular 3D points including noise and crosstalk points. For a static LiDAR sensor, a 3D representation of the background can be created by means of an occupancy grid (voxel grid), in which long-term stable structures emerge. The practical benefit of such a background representation is its applicability for the detection of moving objects (e.g., persons, cars), but it can also be used to detect noise and crosstalk points for evaluation purposes. However, a different filtering method has to be used for dynamic scenes, for a moving sensor system, or for unknown terrain.

**Proposed solution: spatio-temporal filtering of crosstalk points**

For temporal filtering of crosstalk points and noise, we propose to consider only a small number of consecutive point clouds at a time (e.g., 3), which makes this method real-time capable. When filtering point cloud  $c_t$ , we simply compare it to the clouds  $c_{t-1}$  and  $c_{t+1}$ . Given a threshold value  $T$  for maximum distances, a point  $p_j$  of cloud  $c_t$  is only kept if the following condition holds:

$$\exists p_k \in c_{t-1} \cup c_{t+1}: |p_j - p_k| < T.$$

Each point  $p_i$  of cloud  $c_t$ , which does not satisfy this condition, is removed from cloud  $c_t$ . The procedure and its flow chart are illustrated in Figure 3. The threshold  $T$  specifies the maximum distance between the current point  $p_j$  and any neighboring points in the preceding and succeeding clouds. In this way, the filter tolerates small deviations due to the scan pattern or moving objects in the scene.

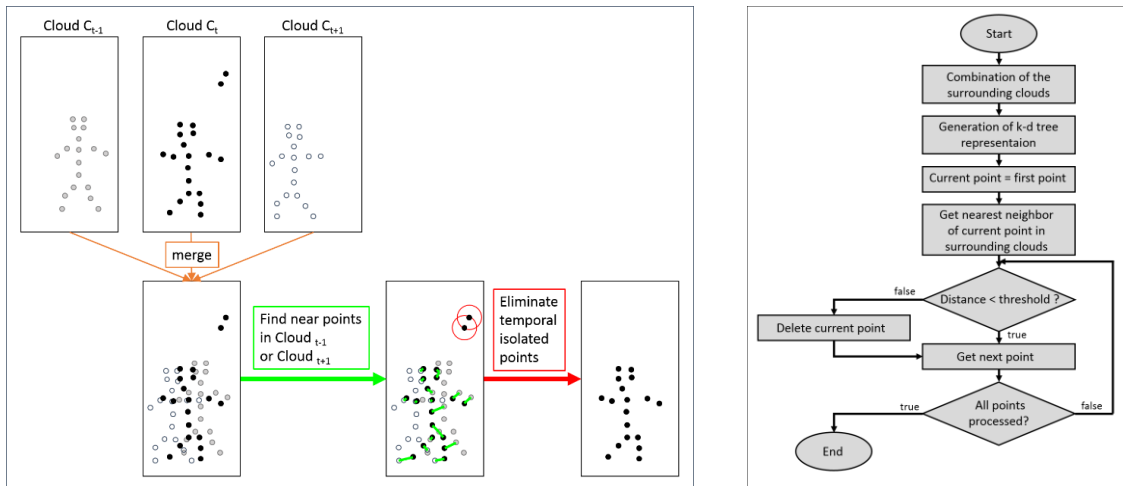


Figure 3: Illustration of the spatio-temporal filtering approach (left) and flow chart of the procedure (right).

This approach eliminates noise and crosstalk points, but it still allows new objects to appear or disappear in the scene (i.e., objects entering or leaving the field of view). Hence, its use is not limited to a non-moving sensor. Our implementation uses a  $k$ -d tree representation of the merged point clouds  $c_{t-1}$  and  $c_{t+1}$  for determination of each point’s neighbors. However, even faster search operations could be performed by exploiting the known scan pattern of the laser scanners (organized point clouds).

**5. EXPERIMENTS AND RESULTS**

**5.1 Experimental platform**

At Fraunhofer IOSB, the experimental multi-sensor vehicle “MODISSA” (Mobile Distributed Situation Awareness) is used for experiments in the contexts of automotive safety, security, and military applications. It is equipped with four LiDAR sensors: two Velodyne HDL-64 sensors above the windshield and two Velodyne VLP-16 sensors above the rear window. Additionally, eight CCD-cameras are placed around the roof’s edges. This arrangement of sensors allows the coverage of the environment around the vehicle, both with LiDAR sensors and video cameras. Furthermore, a pan-tilt-head with an IR-camera and a video camera is placed directly behind the two Velodyne HDL-64 sensors. Figure 4 (left) shows the vehicle and its sensor arrangement. The central clock of MODISSA is provided by an inertial navigation system (INS), which consists of GNSS receivers and an IMU. The INS allows direct georeferencing of the 3D LiDAR data.

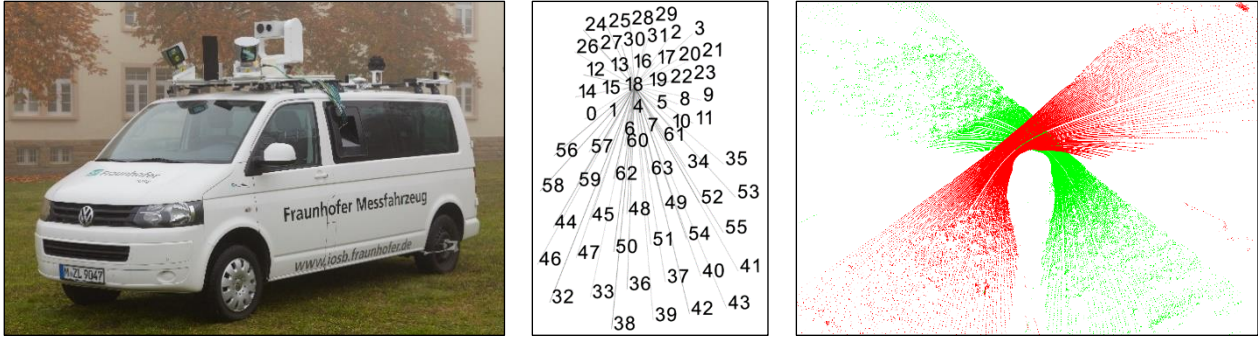


Figure 4: IOSB’s sensor vehicle MODISSA (left), alignment of the 64 emitters of one Velodyne HDL-64 sensor (middle), and top view of 360° scans of both Velodyne HDL-64 sensors (right), green for the right sensor, red for the left sensor.

We only used the two Velodyne HDL-64 sensors of MODISSA for the experiments. Each one is configured to have a rotation frequency of 10 Hz, acquiring 130,000 range measurements (3D points) per rotation with distances up to 120 m. Each sensor has four laser emitter groups of 16 single lasers, and two detector groups of 32 single detectors. Thus, each sensor consists of 64 emitter-detector pairs (i.e., 64 laser rangefinders), subdividing the vertical field of view of  $26.8^\circ$  into 64 scan lines. The laser rangefinders are misaligned to avoid crosstalk caused by the sensor itself (Figure 4 middle).

To avoid direct illumination of the detectors of one sensor by laser pulses of the other one, we placed a black panel between the two sensors, as can be seen in the left image of Figure 4. The rotation axes of both Velodyne HDL-64 sensors have a forward and sideward tilt angle. This arrangement of the sensors provides a high point density in front of the car, where their fields of view overlap (Figure 4 right). In addition, this arrangement allows to measure 3D data at the facades of buildings alongside and behind the car. Due to additional black panels and the mounting angles of the sensors, no direct crosstalk between the Velodyne HDL-64 and the Velodyne VLP-16 sensors in the rear is possible.

## 5.2 Results of spatial filtering of erroneous points caused by crosstalk

In Figure 2, we showed examples for maximal crosstalk effects we discovered during operation of our multi-LiDAR system (MODISSA). For evaluation purposes, a stationary sensor vehicle was used in the first example, and the ground-truth classification of crosstalk points was done by background subtraction. The cloud on the left side of Figure 2 contains 1468 points that are caused by crosstalk (1.31%). For the cloud on the right side of Figure 2, 1138 points (1.53%) can be classified as crosstalk points. The automatic methods described in Section 4 were applied to the sequences of point clouds that contain the respective 360° scans shown in Figure 2.

### “Radius Outlier Removal” filter

This filter needs two parameters: the global search radius and the minimum number of neighboring points. By varying these two parameters and counting the filtered points in both examples, a quantitative comparison of the crosstalk mitigation performance can be made. A qualitative comparison can be done by visual inspection of the resulting clouds. For a selection of parameter values, the numbers of filtered points are given in Table 1.

Table 1: Total number of points removed in the two examples by the “Radius Outlier Removal” filter

	Left cloud of Figure 2 (1468 crosstalk points)			Right Cloud of Figure 2 (1138 crosstalk points)		
	Radius = 0.866	Radius = 1.0	Radius = 2.0	Radius = 0.866	Radius = 1.0	Radius = 2.0
Neighbors = 1	865			452		
Neighbors = 2	1450	1253		1153	780	
Neighbors = 4	2105	1880	442	2570	1851	294
Neighbors = 6		2264	758		2881	535
Neighbors = 8			1102			782

The left side of the following Figure 5 shows the resulting point clouds for a search radius of 1.0 m and the minimum number of neighbors set to 4. It can be seen that the crosstalk points are successfully removed if they occur in a distance where the spacing between the points is wider than or comparable to the search radius (Figure 5a). If the crosstalk effect leads to erroneous points close to the sensor, nearly all these points are kept. Instead, the filter removes regular scene points in greater distances (Figure 5b).

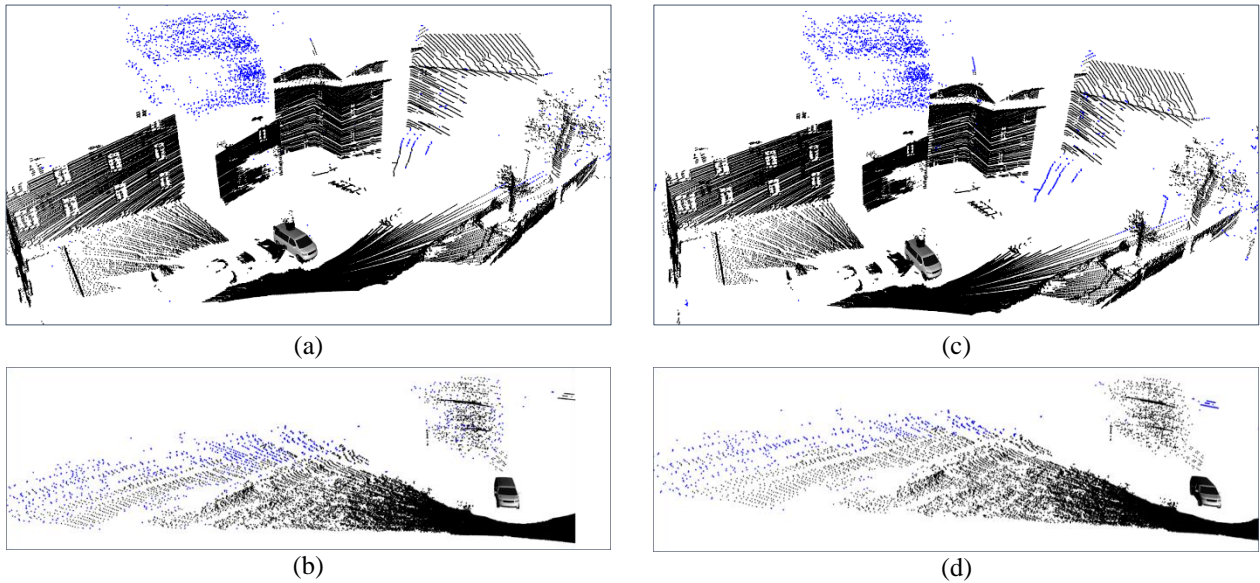


Figure 5: (a), (b): Result of PCL’s “Radius Outlier Removal” filter with search radius set to 1.0 m and minimum number of neighbors set to 4. (c), (d): Result of PCL’s “Statistical Outlier Removal” filter with number of neighbors set to 50 and multiplier  $\alpha$  set to 3.0. Filtered points are shown in blue color.

The example shown in Figure 2 (left) is a single 360° scan/frame that belongs to a sequence of 3200 of such clouds (05:20 minutes). Examining the total sequence of clouds, we can count the number of filtered points per cloud over time. Figure 6 shows the charts for the “Radius Outlier Removal” filter and the “Statistical Outlier Removal” filter. They demonstrate a quite high basic level of point removal for all clouds and peaks where the crosstalk occurs.

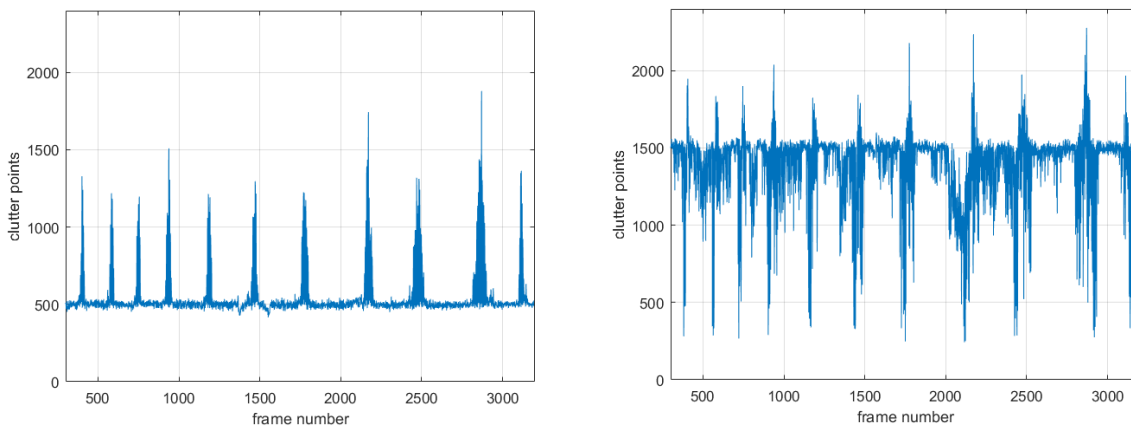


Figure 6: Number of filtered points by “Radius Outlier Removal” (left) and “Statistical Outlier Removal” (right) in a 05:20 minutes sequence of clouds.

### “Statistical Outlier Removal” filter

This filter also needs two parameters: the number  $k$  of neighboring points to be considered for the statistics and the multiplier  $\alpha$  for the standard deviation. By varying the two parameters  $k$  and  $\alpha$  and counting the filtered points in both examples, the following numbers were found (Table 2):

Table 2: Total number of points removed in the two examples by the “Statistical Outlier Removal” filter.

	Left cloud of Figure 2 (1468 crosstalk points)			Right cloud of Figure 2 (1138 crosstalk points)		
	$\alpha = 1.0$	$\alpha = 2.0$	$\alpha = 3.0$	$\alpha = 1.0$	$\alpha = 2.0$	$\alpha = 3.0$
Neighbors = 10	5686	2629	2058	6120	2319	1030
Neighbors = 20	5988	2740	2203	6144	2331	1017
Neighbors = 50	6510	2910	2277	6087	2440	1042
Neighbors = 80	6926	2963	2356	5827	2398	1073

It is obvious from Figure 6 that the basic level of point removal of the “Statistical Outlier Removal” filter is even higher than that of the “Radius Outlier Removal” filter, given the specified parameters. These parameters were set such that the points of buildings in Figure 5c are kept. However, this setting does not remove the crosstalk points in the other example (Figure 5d). The influence of few isolated points on the “Statistical Outlier Removal” filter can be seen in the right chart of Figure 6: Each time when isolated crosstalk points occur, the number of filtered points even decreases, since these isolated points in far distance have a high impact on the statistics. After that, the number of filtered points rises again, depending on the local density of crosstalk points.

### 5.3 Results of temporal filtering of erroneous points caused by crosstalk

#### Background subtraction

In case of a stationary sensor, an easy way to identify erroneous points in a sequence of point clouds is comparing the acquired points to the static background. In our experiments, we used a stationary sensor for evaluation purposes, and we generated an occupancy grid of long-term stable background structures: A voxel cell in this background representation is considered occupied if the number of points accumulated in that voxel over time always exceeds a certain threshold (e.g., more than 5 points per second). The average position of points accumulated in each voxel can be used as a representative 3D point. Figure 7a shows such a representation for parts of the Fraunhofer IOSB’s building and its surrounding area. The occupancy grid with voxel size  $25 \times 25 \times 25$  cm<sup>3</sup> was generated from a sequence of 100 point clouds (10 seconds).

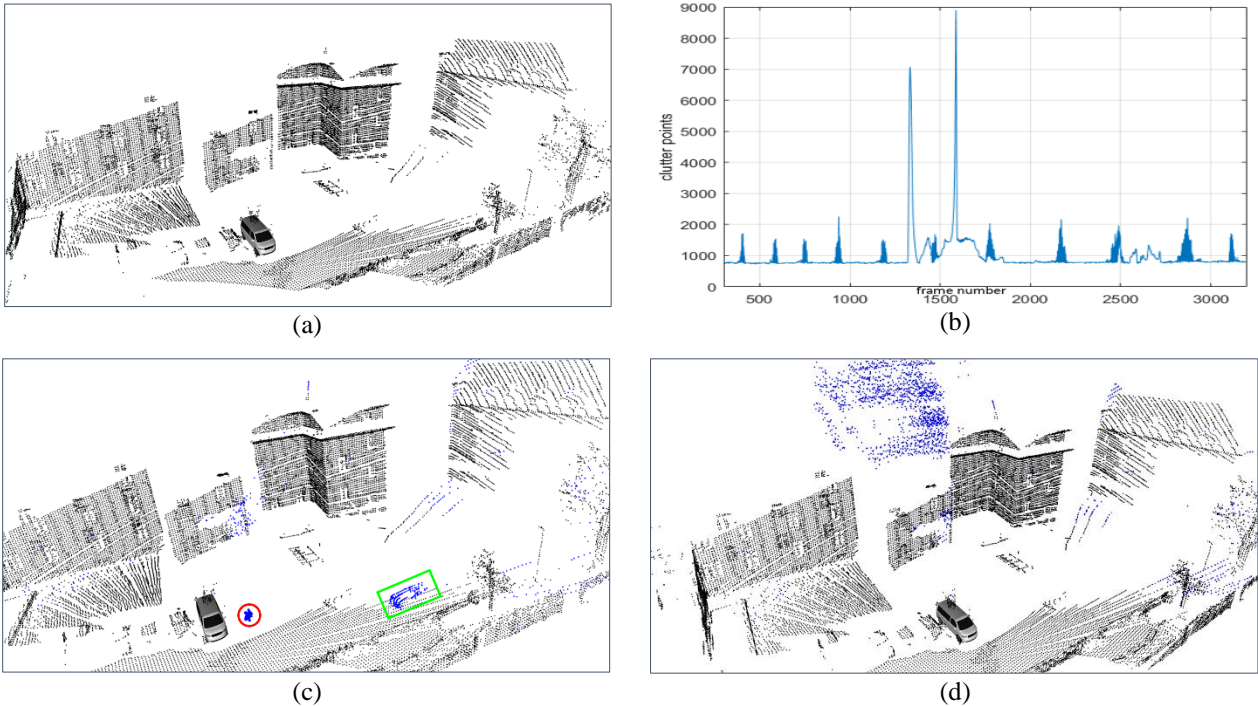


Figure 7: (a) Static background, (b) number of non-background points per cloud of the sequence, (c) blue non-background points of cloud #1560 showing a person and a car, (d) blue non-background points of cloud #2869 caused by crosstalk.



The comparison of the background representation to each point cloud of the sequence allows the detection of non-background points (background subtraction). These non-background points could either be changes due to movements in the environment (e.g., leaves in the wind, walking people, or moving vehicles), noise, or points resulting from crosstalk effects. The chart in Figure 7b shows the number of non-background points for each cloud of the sequence (3194 consecutive 360° scans of one of the two Velodyne HDL-64 laser scanners). Besides a basic level of non-background points (e.g., noise), their number increases notably and quite regularly from time to time. These peaks are caused by crosstalk points, as they are shown in blue color in Figure 7d. The reason for their oscillating appearance is a slight difference in the rotation frequencies of both laser scanners, leading to periodically changing geometrical constellations of one laser scanner’s emitters and the other laser scanner’s detectors. The broader and more prominent peaks between cloud #1300 and cloud #1750 can be explained by a walking person and a moving car in the scene (red circle and green box in Figure 7c).

**Results of the proposed method: spatio-temporal filtering of crosstalk points**

We tested the aforementioned background-subtraction for evaluation purposes only, since the actual filtering method is intended to be usable on a moving sensor carrier and in unknown terrain. Our own approach for mitigation of crosstalk effects, as it was introduced in Section 4.2, only needs three consecutive clouds at a time to perform the temporal filtering. With a time delay of only one 360° rotation of the scanner head, this approach can be performed synchronously with the data acquisition.

For the experiments, the search radius  $T$  was set to 0.866. Figure 8d shows the chart of the removed points per cloud of the sequence. The basic level of unnecessarily filtered points is definitely lower than that of the previous approaches, while the peaks indicating crosstalk effects are clearly visible. As requested, moving objects in the scene (e.g., cars, persons) are not removed by the filter (see examples in Figure 8b), but points caused by crosstalk effects are reliably identified and removed in both examples of Figure 2, as it can be seen in Figure 8a and Figure 8c. It is evident from Figure 8c that even sparse ground points in greater distances are preserved.

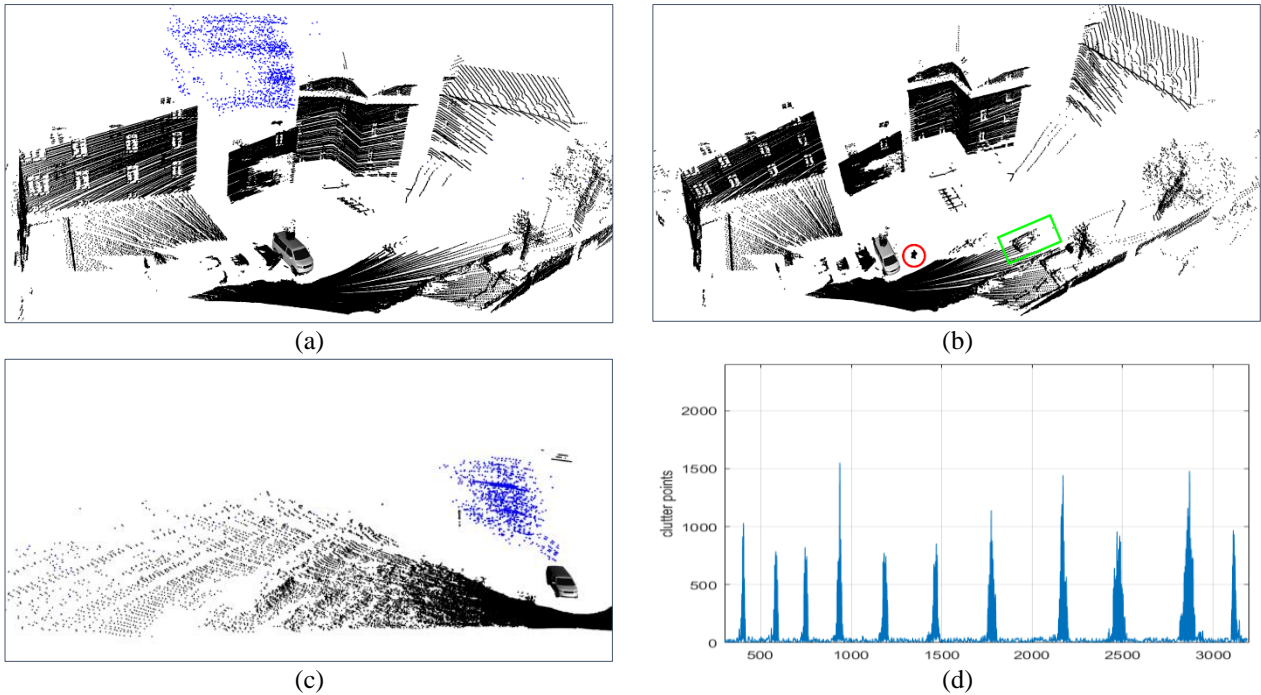


Figure 8: Results of spatio-temporal filtering: (a) crosstalk points detected in cloud #2869, (b) moving objects are preserved, (c) crosstalk points are filtered, sparse ground points are kept, (d) number of filtered points per cloud in the sequence.

**5.4 Possible sources of crosstalk effects**

In Section 3, we described how crosstalk effects arise out of an unintended propagation of laser pulses between different LiDAR sensors. During operation of our multi-LiDAR system MODISSA, we usually detect a notable amount of crosstalk points occurring in quite regular time intervals. As mentioned before, the reason for this periodic behavior are slightly

different rotation frequencies of the two laser scanners. In addition, the majority of crosstalk points can typically be found in nearly the same direction (behind the vehicle). Obviously, most crosstalk effects we observe are self-induced by MODISSA, and the source is a reflecting object on the vehicle itself. To determine the reflecting object, we converted the range data of single  $360^\circ$  scans into range images according to azimuth and elevation. Figure 9 shows such a range image of the scene in Figure 2a, in which the gray value of each pixel represents the measured distance to the reflecting surface. The sinusoidal shape of the range image is caused by the tilted installation of the sensor (see Figure 4a).

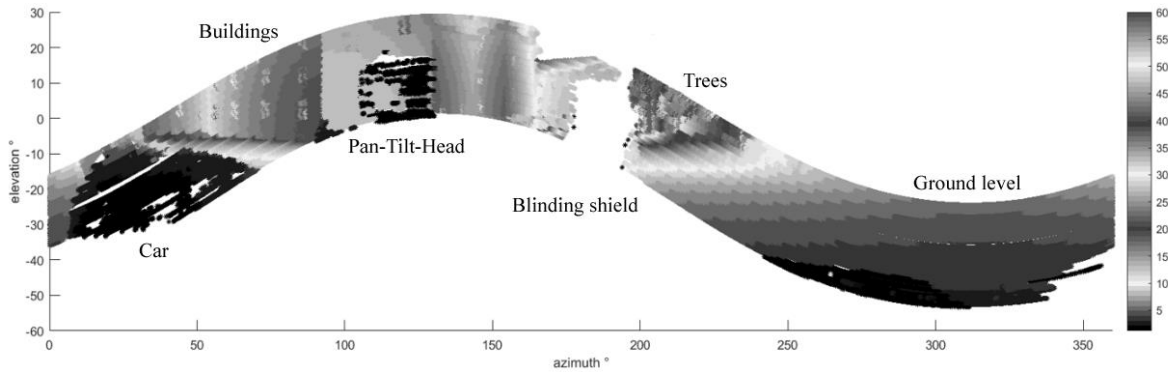


Figure 9: Exemplary range image of a  $360^\circ$  scan of one of MODISSA’s Velodyne HDL-64 laser scanners. The data correspond to the scene shown in Figure 2a. The gray levels represent distances to the sensor.

After the detection of erroneous points with the proposed method, their position in the range image indicates that the object causing most crosstalk effects in our system is the pan-tilt-head (PTH) mounted on MODISSA’s roof (see Figure 11a). The two laser scanners Velodyne HDL-64 and the PTH form an isosceles triangle, with a distance of about one meter of the PTH to each of the laser scanners. Although this geometrical constellation is very specific to our sensor system, it demonstrates that multi-LiDAR systems are prone to crosstalk effects. As long as all LiDAR sensors are part of the same system, another simple way to remove these crosstalk points could be masking out the problematic parts of the field of view (in our case: the sector where the PTH is located). In order to avoid crosstalk points at all, a precise control of the rotation speed of the laser scanners could be a solution, such that geometrical constellations causing crosstalk can never occur. However, such measures are not sufficient if some LiDAR sensors in the scene are not under own control, or if the reflecting objects causing crosstalk are not part of the own sensor carrier.

In view of the latter case, an additional experiment was conducted to quantify the susceptibility of our multi-LiDAR system to crosstalk caused by typical scene objects. For comparisons, we first recorded a dataset in an open field. In the second run, three persons were standing in front of the sensor vehicle. We found crosstalk points in both recorded sequences, and we subdivided them based on the sector they occur. As expected, most crosstalk points are caused by the PTH of MODISSA (blue curves in Figure 10), but some crosstalk points can even be traced back to the ground surface in front of the vehicle. With the three persons standing in that direction, these peaks get notably higher (orange curves in Figure 10).

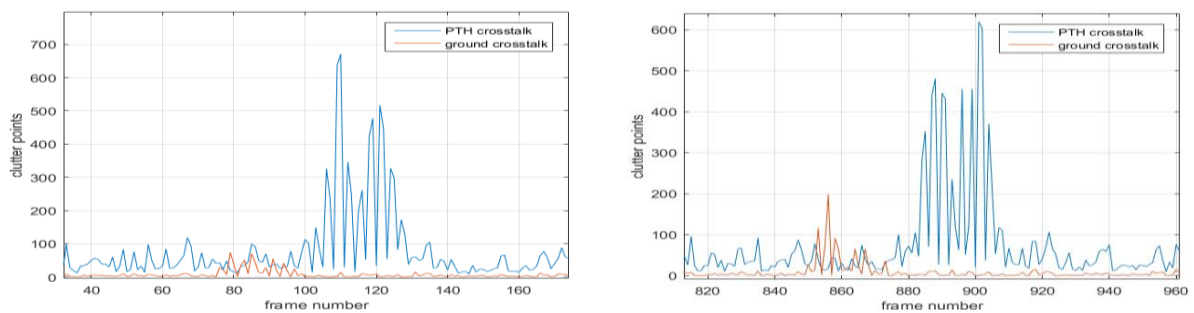


Figure 10: Left: Number of particular crosstalk points in an open field. Right: Same scene, but with three persons in it.

Figure 11a shows the range image of a single  $360^\circ$  scan in which crosstalk effects are caused by the PTH. The detected crosstalk points are marked in red color. In the same sequence but at other times, crosstalk points occur due to scene objects in front of the vehicle (Figure 11b).

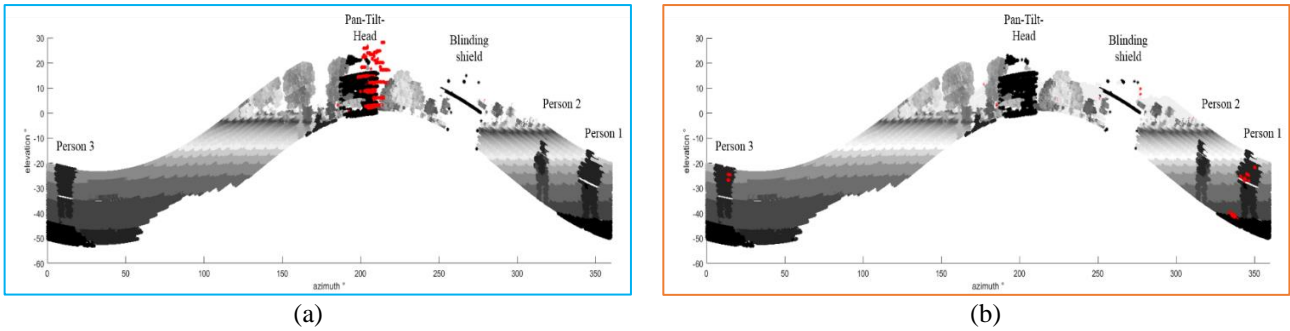


Figure 11: Range images of the scene with three persons in front of MODISSA. Detected crosstalk points are marked in red color. (a) Crosstalk caused by the PTH in cloud #901, (b) crosstalk caused by persons in cloud #856.

### 5.5 Impact on the detection of small moving objects

The detection of mini and micro UAVs (unmanned aerial vehicles) with 360° scanning LiDAR sensors is a challenging task due to the small size and the unpredictable and fast movement of the targets. At a medium distance range, typically less than five points per scan hit the target. Crosstalk points and other noise have high potential to mislead any detection methods for UAVs. Our spatio-temporal filtering approach is able to remove crosstalk points and noise while keeping moving objects. The example on the right side of Figure 2 is taken from a sequence of point clouds, which we acquired during a measurement campaign to investigate the potential of LiDAR sensors for the detection of UAVs [1]. A small flying UAV was present in the scene while MODISSA was moving (red circle in Figure 12).

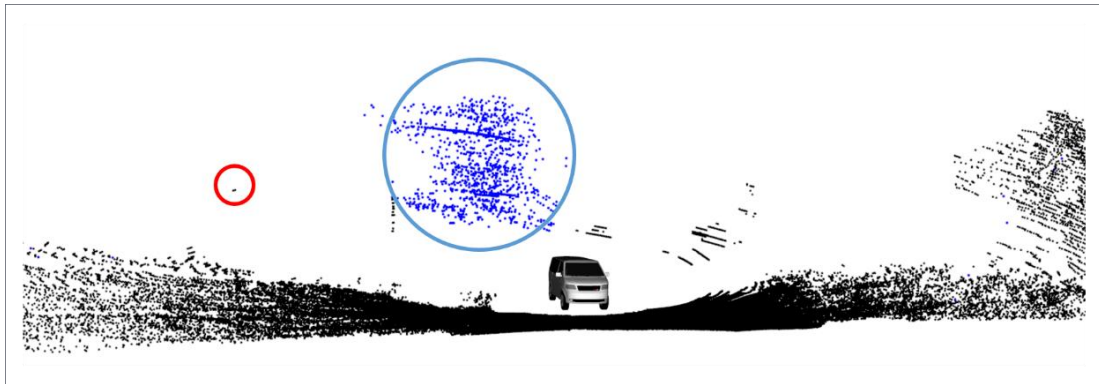


Figure 12: Example of a 3D point cloud acquired by one of MODISSA's Velodyne HDL-64 laser scanners during field trials for UAV detection. Filtered crosstalk points are marked in blue color; the UAV-related 3D points are kept (red circle).

Data recorded during this field trial consist of sequences of eight different scenarios with more than 39,000 point clouds in total. The proposed filtering method was applied to these data as a preprocessing step for UAV detection and tracking. Since the UAVs flew comparatively slowly in these examples, we observed no filtering of UAV-related points. However, it is obvious that small high-speed UAVs are likely to be filtered from the data when using the proposed method, depending on the filter's parameter settings, the scanning speed of the sensors, and the speed of the UAV. One area of future work could be an investigation of these relations in a more quantitative manner.

## 6. CONCLUSIONS

During operation of our multi-LiDAR sensor system MODISSA, we usually observe periodically occurring mutual interferences between the laser scanners, leading to erroneous 3D points in the data. For our specific system, these periodic crosstalk effects can be traced back to slightly varying rotation speeds of the two laser scanners and a reflecting object on the sensor carrier itself (PTH). Nevertheless, our experiences demonstrate that multi-LiDAR systems are prone to crosstalk effects in general.

We believe that technical improvements of LiDAR sensors will be the solution of choice for crosstalk mitigation or avoidance in future. However, for sensors currently available on the market, we propose a data-based filtering method to detect and remove crosstalk points. Software packages like the “Point Cloud Library” offer standard methods for outlier removal by spatial filtering, but these filters tend to incomplete filtering of dense crosstalk points, while removing small objects and sparse scene points in larger distances.

In this paper, we presented a data-based spatio-temporal filtering method for the mitigation of crosstalk effects. This approach only needs three consecutive overlapping point clouds at a time to perform the temporal filtering. With a time delay of only one scanning cycle, this approach can be performed synchronously with the data acquisition if an efficient implementation is used. In our experiments, we applied the proposed method to LiDAR data acquired in urban terrain and in an open field scenario. The results show that crosstalk points can be reliably detected and filtered, provided that the movements of the sensor carrier and objects in the scene (cars, persons, UAVs, etc.) are slow in comparison to the scanning speed of the LiDAR sensors.

## REFERENCES

- [1] M. Hammer, M. Hebel, B. Borgmann, M. Laurenzis, M. Arens, “Potential of LiDAR sensors for the detection of UAVs”, *Proc. SPIE 10636*, 1063605 (2018).
- [2] L. Mu, T. Xiangqian, S. Ming, Y. Jun, “Research on Key Technologies for Collision Avoidance Automotive Radar”, *Proc. Intelligent Vehicles Symposium*, 233-236 (2009).
- [3] M. Goppelt, H.-L. Blöcher, W. Menzel, “Analytical investigation of mutual interference between automotive FMCW radar sensors”, *Proc. 6th German Microwave Conference*, 312-315 (2011).
- [4] T. Schipper, S. Prophet, M. Harter, L. Zwirello, T. Zwick, “Simulative Prediction of the Interference Potential Between Radars in Common Road Scenarios”, *IEEE Transactions on Electromagnetic Compatibility* 57 (3), 322-328 (2015).
- [5] M. Kunert, “The EU project MOSARIM, A general overview of project objectives and conducted work”, *Proc. of the 9<sup>th</sup> European Radar Conference*, 1-5 (2012).
- [6] M. Ahrholdt, F. Bodereau, Chr. Fischer, M. Goppelt, R. Pietsch, A. John, A. Ossowska, M. Kunert, “D12.1 - Study report on relevant scenarios and applications and requirements specification”, the MOSARIM Consortium, [<https://cordis.europa.eu/docs/projects/cnect/1/248231/080/deliverables/001-MOSARIMDeliverableD121V11.pdf>] (2010).
- [7] M. Hebert, E. Krotkov, “3-D Measurements From Imaging Laser Radars: How Good Are They?”, *Proc. International Workshop on Intelligent Robots and Systems IROS '91*, 359-364 (1991).
- [8] G. Kim, J. Eom, Y. Park, “Investigation on the occurrence of mutual interference between pulsed terrestrial LIDAR scanners”, *2015 IEEE Intelligent Vehicles Symposium (IV)*, 437-442 (2015).
- [9] Velodyne Lidar Inc., D. S. Hall, P. J. Kerstens, “Multiple Pulse, LIDAR Based 3-D Imaging”, patent US20170219695A1, [<https://patents.google.com/patent/US20170219695A1/en>] (2016).
- [10] “Facet Technology Launches Its Safe and Secure LiDAR Crosstalk Elimination Licensing Program”, press release, [<https://www.pr.com/press-release/703312>] (2017).
- [11] Y. Lipman, D. Cohen-Or, D. Levin, H. Tal-Ezer, “Parameterization-free Projection for Geometry Reconstruction”, *ACM Trans. Graph.* 26 (3), 22 (2007).
- [12] H. Huang, D. Li, H. Zhang, U. Ascher, D. Cohen-Or, “Consolidation of Unorganized Point clouds for Surface Reconstruction”, *ACM Trans. Graph.* 28 (5), 176:1-176:7 (2009).
- [13] X.-F. Han, J. S. Jin, M.-J. Wang, W. Jiang, L. Gao, L. Xiao, “A review of algorithms for filtering the 3D point cloud”, *Signal Processing: Image Communications* 57, 103-112 (2017).
- [14] R. B. Rusu, S. Cousins, “3D is here: Point Cloud Library (PCL)”, *IEEE International Conference on Robotics and Automation*, 1-4 (2011).
- [15] R. B. Rusu, Z. C. Marton, N. Blodow, M. Dolha, M. Beetz, “Towards 3D point cloud based object maps for household environments”, *Robotics and Autonomous Systems* 56, 927-941 (2009).